Astron. Astrophys. 71, 205—210 (1979)

ASTRONOMY AND ASTROPHYSICS

The Electron Temperatures of H II Regions Determined from Radio Recombination Line Observations at 22 GHz

T. L. Wilson, J. Bieging, and W. E. Wilson

Max-Planck-Institut für Radioastronomie, Auf dem Hügel 69, D-5300 Bonn, Federal Republic of Germany

Received November 21, 1977; revised May 8, 1978

Summary. This paper presents radial velocities, line widths and LTE electron temperatures obtained from the H 66α line together with continuum measurements for 15 strong H II regions measured at 22.4 GHz with a resolution of $\sim$43″. The ratio of the intensities of the H 83β to the H 66α lines, measured for 5 sources, is consistent with LTE. Hence the effect of stimulated emission is small, and the true and LTE electron temperatures are directly related. The average LTE electron temperature for the sources in the survey is 7900 K. Our LTE electron temperatures are in excellent agreement with the H 66α data for six sources measured by Waltman and Johnston (1973) with an angular resolution of 2.3′. We conclude that there are no large gradients in the electron temperature for these sources and the effects of source geometry (Lockman and Brown (1976)) are also small at 22.4 GHz. We compare these data with the H 109α and H 137β data of Churchwell et al. (1977), measured with a 2.6′ resolution. The agreement between the H 109α and H 66α electron temperatures (calculated assuming Local Thermodynamic Equilibrium) is surprisingly good, whereas the LTE electron temperatures calculated from the H 137β line are, on the average, 1800$\pm$600 K higher than the LTE electron temperatures obtained from the H 66α line data. Any theoretical explanations of these results can be tested only for Orion A, for which the most data are available. The new H 66α and H 109α data require a modification of the Brocklehurst and Seaton model (1972), in which substantial clumping must be included. Our results are not extensive enough to fully test the proposed gradient in electron temperatures of H II regions with distance from the galactic center but the H 66α data are consistent with such a gradient.

Key words: recombination lines — LTE electron temperatures — H II regions

Send offprint requests to: T. L. Wilson

The observations of radio recombination lines at frequencies higher than 20 GHz are valuable because: (1) the continuum optical depth of the sources is low, so that the recombination line emission is not affected by stimulated emission and the true electron temperatures of H II regions can be calculated accurately; (2) the telescope beam size is smaller than at lower frequencies, so that structure in H II regions can be resolved; (3) at high frequencies, the dense cores of compact H II regions, such as W 3 (OH) are optically thin, so the properties of high density ionized gas can be investigated and (4) the effect of stark broadening of recombination lines will be negligible. As emphasized by Brown et al. (1978) the electron temperatures obtained from recombination lines measured at high frequencies will refer to the densest parts of the H II regions. Previous surveys of the radio recombination lines of hydrogen at frequencies above 20 GHz, made by Berulis et al. (1975) and Waltman and Johnston (1973), had angular resolutions of 2–3′. These groups reported electron temperatures (calculated assuming Local Thermodynamic Equilibrium, hereafter LTE) of 7000–8000 K, considerably lower than the generally accepted value of 10^4 K. The motivation for the present survey was: (1) to reduce the uncertainties in the LTE electron temperatures measured previously by taking advantage of the large collecting area of the 100 m telescope, and (2) to use the $\sim$43″ beam of the telescope to investigate conditions in the compact cores of H II regions.

Observations

The observations were made with the 100 m telescope of the Max-Planck Institut für Radioastronomie in November 1976. At 22.364 GHz, the rest frequency of the H 66α line, the full width to half power of the telescope beam is $\sim$43″. The aperture and beam efficiencies of the telescope are a fairly strong function of elevation at this frequency. In the zenith the aperture efficiency is 0.3 and the beam efficiency is 0.4, for the inner 80 m of the telescope. The receiver was a cooled parametric

Table 1. Continuum and H 66α line data

(1) Source Name	(2) Source coordinates R.A. (1950) h m s	(3) Decl. (1950) o ' "	(4) Observed Source Size θ_α (")	(5) θ_δ (")	(6) Source Flux Density S_ν (Jy)	(7) Velocity V_{LSR} (km s^{-1})	(8) Full Width to Half Power $\Delta V_{1/2}$ (km s^{-1})	(9) Line to Continuum Ratio T_L/T_c a)	(10) Electron Temperature LTE T_e (K)	(11) Model T_e b) (K)	(12) Distance from Galactic Center R_{GC} (kpc)
W3 A	02 21 57	+61 52 41	54	60	30	-39.1±0.2	27.7±1.6	0.23±0.02 (2)	8400±1200	8700	12
W3 B	02 21 50	+61 52 34	--	51	--	-39.5±0.2	26.0±1.0	0.24±0.04 (3)	8500±1300	9000	12
Orion A	05 32 47	-05 25 23	136	195	375	- 1.4±0.6	25.8±0.5	0.25±0.01 (2)	8200± 300	8500	10.5
Ori A (1.6'S)	05 32 50	-05 26 49	--	--	--	- 2.2±0.2	26.2±0.4	0.26±0.01 (1)	7700± 500	----	10.5
NGC 2024	05 39 13	-01 56 15	156	84	36	6.4±0.2	22.4±0.5	0.34±0.01 (1)	7200± 500	6800	10.5
Mon R2	06 05 19	-06 22 29	45	45	8	12.1±0.5	27.6±1.4	0.21±0.01 (1)	9000± 800	9300	∿11
Sgr B2	17 44 10	-28 22 12	48	∿54	24	61.7±0.4	35.0±1.2	0.21±0.01 (1)	7500± 500	8500	0.2
W33	18 11 18	-17 56 32	43	43	27	36.2±0.2	32.3±0.5	0.28±0.01 (1)	6100± 300	6900	5
M17	18 17 33	-16 13 23	93	183	216	15.4±0.3	31.4±0.7	0.21±0.01 (1)	8000± 300	8200	8
W49 (5)	19 07 50	+09 01 29	70	48	24	6.3±0.1	27.9±0.4	0.25±0.02 (1)	7700± 600	7900	9.5
W49 (6)	19 07 58	+09 00 18	42	51	8	10.6±0.3	34.0±0.8	0.20±0.01 (1)	7800± 500	8200	9.5
W51 B	19 21 15	+14 24 13	60	60	13	66.2±0.6	27.1±0.7	0.23±0.03 (1)	8500± 800	8000	8
W51 D	19 21 22	+14 25 19	81	57	36	56.4±0.1	31.0±0.6	0.26±0.01 (2)	6800± 300	6800	8
W51 E	19 21 24	+14 24 52	54	66	55	58.0±0.2	29.5±0.4	0.24±0.02 (2)	7400± 800	8200	8
K3-50	19 59 58	+32 25 53	43	43	3	-16.5±0.6	32.2±1.7	0.21±0.02 (1)	8000± 600	8400	10
DR 21	20 37 14	+42 08 55	45	45	21	- 0.7±0.3	32.7±3.0	0.19±0.02 (2)	8400± 500	9500	10

a) in parentheses are the number of independent observations included in the determination of T_e
b) corrections to the LTE electron temperatures were made assuming that the H II regions are uniform density, isothermal spheres, using the line and continuum data in Table 1 and the b_n and β values of Brocklehurst (1970). We emphasize that the model T_e's are based only on the 22 GHz data. The model electron temperatures are related to the LTE electron temperatures by Eq. (3), which is solved iteratively

amplifier which typically had a noise temperature of 160 K, referred to the feed horn. Atmospheric attenuation increased the system noise by between 40 K and 150 K, depending on weather conditions and source elevation. The spectrometer was a 384-channel autocorrelator with a 10 MHz bandwidth, giving a spectral resolution of 31.5 kHz (=0.4 km s^{-1}). Spectral line measurements were made by switching between positions separated by 5^m of time in Right Ascension, with on-source and off-source integration times of 5 min, so that the source and reference spectra covered the same range of azimuth and elevation.

Continuum measurements were made by scanning across the source in both right ascension and declination. The receiver was stabilized against gain drifts by load switching, except in the case of K 3–50 and DR 21. These two sources are small enough to permit beam switching (the separation of the beams is 112″), which provided excellent cancellation of baseline variations caused by the weather. For the other, more extended sources, the principal source of uncertainty in the measured continuum intensities is the fluctuation in the zero level because of the weather.

Since the main purpose of these observations was to determine the ratio of the integrated line intensity to the continuum intensity, the continuum and line measurements were made at nearly equal elevations. In general, a source was first scanned to measure the continuum intensity; then the spectrum was obtained in one or more pairs of 5^m integrations. If the source moved through a significant range of elevation angles during the spectral integration, a continuum scan was repeated at the end of the spectral measurement and the adopted continuum intensity was taken as a mean value. This procedure was used for both the H 66α and the H 83β line measurements. For our determination of the H 83β/H 66α ratio the effects of weather, telescope elevation, etc., were eliminated by requiring that the continuum temperatures measured in conjunction with the H 66α or H 83β lines are equal, and adjusting the line temperatures accordingly.

Results

H 66α Line

The basic observational data for the sources are summarized in Table 1. The source sizes, θ_α and θ_δ, are the widths at half-maximum intensity measured by hand from the continuum scans, and have not been corrected for broadening by the ∼43″ telescope beam. The uncertainties in the source sizes are ∼5″. The flux density was determined from the peak intensity (corrected for elevation) and the measured size. The flux density scale was determined by scans across either NGC 7027 or W 3 (OH), which were assumed to have a flux densities of 6.0 Jy or 3.5 Jy at 22.4 GHz respectively. The uncertainties in the flux densities are estimated to be 30%.

Table 2. H 83β line results

(1) Source Name	(2) V_{LSR} (km s^{-1})	(3) $\Delta V_{1/2}$ (km s^{-1})	(4) $\frac{T_L(H83\beta)\ \Delta V_{1/2}\ (H83\beta)}{T_L(H66\alpha)\ \Delta V_{1/2}\ (H66\alpha)}$
W3 A	-37.5±0.4	30.2±1.2	0.23±0.03
W3 B	-40.0±0.5	27.5±1.3	0.26±0.03
Orion A	+ 0.4±0.6	25.5±0.4	0.27±0.02
NGC 2024	+ 6.3±1.0	25.6±0.6	0.32±0.05
W51 E	+57.5±0.2	31.3±0.7	0.30±0.01

[a] The LTE value of the β to α ratio is 0.276

Table 3. Comparison of electron temperatures derived from H 66α and H 56α observations

Source	LTE Electron Temperature, T_e*		
	(H56α) (Berulis et al.)	(H66α) (Waltman & Johnston)	(H66α) (This paper)
W3	8260±600	8100±1700	8400±1200[a]
Orion A	7670±500	7800± 800	8200± 300
NGC 2024	8400±650	7000±1300	7200± 500
Sgr B2	-- --	-- --	7500± 500
M17	-- --	7150± 800	8000± 300
W49	-- --	7150±1300	7800± 600[a]
W51	6960±500	7450±1000	7300± 500[a]
DR21	7020±700	-- --	8400± 500

[a] Average electron temperature, weighted by the continuum temperatures of the components in the region

The intensity, center velocity V (relative to the LSR) and the full width to half power of the H 66α line were determined for each source by a gaussian fit to the spectrum. The results were compared with visual estimates of these parameters from the plotted spectra. The agreement was generally very good, except in a few cases where the spectral baseline was curved. The uncertainties quoted in Table 1 reflect both the formal errors of the gaussian fit and the degree of consistency between fitted and directly measured values. Because, as discussed earlier, the measured line and continuum intensities are functions of source elevation, we do not give in Table 1 a value for the peak line temperature alone. Instead we give the ratio of the line to continuum antenna temperature, which is the relevant parameter for calculating an electron temperature. We define R as

$$R=\frac{T_L}{T_c}\cdot\Delta V_{1/2}, \tag{1}$$

where (T_L/T_c), the line-to-continuum ratio, is given in Col. 9 of Table 1. The full width to half power $\Delta V_{1/2}$, is given in Col. 8 of Table 1. The LTE electron temperature of the H II region, T_e*, which produces the observed H 66α emission is given by

$$T_e^*=\frac{1.84\ 10^5\ (N^+/N_e)}{R\left\{\frac{3}{2}\log T_e^*-2.66\right\}}=\frac{1.84\ 10^5\ (N^+/N_e)}{Rg(T_e^*)}. \tag{2}$$

Eq. (2) must be solved iteratively. $g(T_e^*)$ is the Gaunt factor. (N^+/N_e) is the ratio of proton density to electron density. Except for NGC 2024, we have taken the ratio of singly ionized helium to hydrogen to be 0.08. Then (N^+/N_e) is $(1.08)^{-1}$. For NGC 2024, where the ionized helium to ionized hydrogen ratio is 0.03 [Churchwell et al. (1977)], we have used $(1.03)^{-1}$. Values of T_e*, the LTE electron temperature, are listed in Col. 10 of Table 1. The quoted uncertainties reflect primarily the uncertainty of the continuum temperature, since the error in the line data is small. Finally, the distance of the H II region from the center of the galaxy is given in Col. 12. Distances are based in most cases on kinematic determinations using the measured radial velocities. Distance estimates for sources with large non-circular velocities, such as Sgr B 2 and W 33 are discussed in notes and comments on the individual sources, which are given in the Appendix.

H *83 β Line*

For five sources, the H 83β line was also observed in the same manner as the H 66α line. The ratio of the integrated intensities of these two lines furnishes a measure of the departure from LTE in the ionized gas. The results are summarized in Table 2. The derived center velocities and line widths agree to within 1 or 2σ with the corresponding values for the H 66α line from Table 1. The value of the β- to α-intensity under LTE conditions is 0.28. The values for this ratio in Col. 4 are consistent with the LTE value to within 1σ for W 3 B, Orion A, and NGC 2024, and to within 2σ for W 3 A and W 51 E. These data indicate that, at least in these sources, the recombination lines at 22 GHz are formed very nearly under conditions of thermodynamic equilibrium.

Corrections for Stimulated Emission

Although the H 66α lines are very nearly formed in LTE, one can estimate the true electron temperature, T_e, using corrections for non-LTE effects, from

$$T_e=b_nT_e^*\left\{(g(T_e^*)/g(T_e)\right\}\left(1+\tfrac{1}{2}(1-\beta)\tau_c\right), \tag{3}$$

where b_n is the departure coefficient, β is the stimulated emission term, τ_c is the continuum optical depth at the line frequency, and g is the Gaunt factor. Eq. (3) must be solved iteratively because the values of b_n and β depend on the true electron temperature and electron density. We have estimated these source parameters from the model calculation computer program of Walmsley and Churchwell. The model is based on: (1) The assumption that the H II region is isothermal,

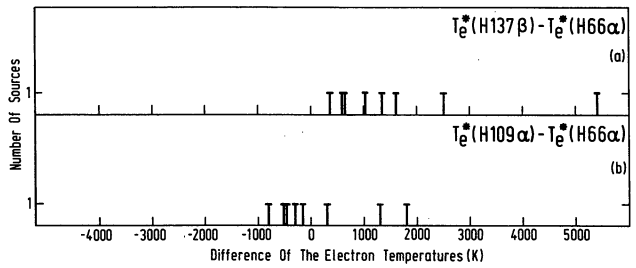

Fig. 1. a The distribution of the difference between the H 137β and H 66α LTE Electron Temperatures. The source at the extreme right, with a difference of 5400 K, is Sgr B 2, and the source with a difference of 2500 K is DR 21. **b** A histogram of the difference between the H 109α and H 66α LTE Electron Temperatures. The source which has a difference of 1900 K is Sgr B 2, and the source with a difference of 1300 K is DR 21.

has a uniform density and is spherical, and (2) the line and continuum parameters in Table 1 (we have used the source sizes given in Col. (4) and (5) after correcting for the telescope beam assuming gaussian source and beam shapes), and (3) the b_n and β values of Brocklehurst (1970).

The angular sizes of W 3 B, W 33, W 49(6) and K 3–50 are considerably smaller than our beam and we have used sizes obtained from aperture synthesis maps. The references from which these sizes were obtained are listed in the Appendix. The LTE electron temperature at the position 1.6′ south of the peak of Orion A was not corrected. The amount of the correction depends on the geometry, for example, Pauls and Wilson (1977) assumed that Orion A had a gaussian source shape and found that no correction for stimulated emission was required at 22 GHz, in contrast to the 4% correction given in Table 1. We conclude that geometry can affect non-LTE corrections by 5%. The corrections for stimulated emission are less than 13% for the sources we have observed, and we will use the LTE electron temperatures in the following discussions.

Discussion

Comparisons with Other Observations of High Frequency Recombination Lines

In Table 3 we compare our values for T_e^* with those surveys made at high frequencies which include more than 1 source, and where the errors in T_e^* are less than 20%. Berulis et al. (1975) give T_e^* results for the H 56α line (rest frequency = 36.46 GHz), and Waltman and Johnston list T_e^* values for the H 66α line. On the average our values of T_e^* are slightly larger than those obtained in either of the other two surveys. However, with the exception of the T_e^* value for DR 21, the results agree at the 1σ level. Considering the difference in beamsize (the other surveys had telescope beams $\geqq 2'$), the agreement is very good. The agreement with the survey of Waltman and Johnston (made with a resolution of 2.3′), makes it unlikely that systematic spatial gradients in the electron temperatures in H II regions and the effects of source geometry [emphasized by Lockman and Brown (1976)] are present for these sources at 22.4 GHz.

Table 4.

(1)	(2)	(3)	(4)	(5)	(6)	(7)
Source	H83β/H66α Ratio	H137β/H109α Ratio	T_e^*(H66α) (This paper)	T_e^*(H109α) (Churchwell et al.)	T_e^*(H137β) (Churchwell et al.)	T_e (Model) [d]
W3	0.24±0.02 [a]	0.20±0.01	8400±1200	7920	10000	10910
Orion A	0.27±0.02	0.23±0.003	8200± 300	8050	9240	11170
NGC 2024	0.32±0.01	0.30±0.01	7200± 500	7510	7560	8810
Sgr B2		0.19±0.01	7500± 500	9300	12900	13620
M17		0.21±0.005	8000± 300	7550	9060	11380
W49		0.20±0.006	7800± 600 [c]	7480	9150	10420
W51	0.30±0.01 [b]	0.22±0.007	7300± 500	6530	7970	9310
DR21		0.24±0.02	8400± 500	9790	10920	16690

[a] Unweighted average for W 3 A and W 3 B.
[b] Result for W 51 E only.
[c] Average electron temperature, weighted by source continuum of components in region.
[d] These model T_e's are based only on 5 GHz data.

Comparison of T_e^* Values from H 137β, H 109α, and H 66α Data

We compare T_e^* values from the H 137β and H 109α line survey of Churchwell et al. (1977) with our results in Table 4. A plot of the difference between the H 66α T_e^* and the T_e^*'s from the H 137β and H 109α data are given in Figs. 1a and 1b. The average value of the T_e^* from the H 109α line is 200 K larger than the average T_e^* from the H 66α line. This difference is smaller than the 1σ errors in either set of data. On the other hand, the T_e^* from the H 137β line data is 1800 K larger than the T_e^* from the H 66α line. This difference is more than twice the standard error of the mean, 600 K.

The two sources with the largest differences in the LTE electron temperatures at 5 and 22 GHz, both for the H 137β and H 109α lines, are Sgr B 2 and DR 21. Continuum optical depth effects must play a large role. Excluding these two H II regions, the LTE electron temperatures obtained from the H 137β data are 1000 $\pm$200 K (uncertainty is the error of the mean) larger than the LTE electron temperatures obtained from the H 66α line data. Although the 2.6′ resolution of the H 137β and H 109α data is 15 times the area of the ~43″ beam used to take the H 66α results, we have previously argued that large temperature gradients are not present at 22 GHz, and hence one can compare these data. For the sources in Table 4, the average width of the H 66α line is ~3 km s^{-1} smaller than the average width of the H 109α line. Such a difference can be

explained by the large difference in the angular resolution in these surveys, and mass motions in the H II regions. However the average of the widths of the H 137β lines of the sources in Table 4 is $\sim$4 km s^{-1} larger than the average of the widths of the H 109α lines. Since these data were taken with the same resolution at the same frequency, mass motions of the ionized gas cannot account for the difference. As pointed out by Churchwell et al., pressure broadening is probably the cause.

The ratio of the H 137β to H 109α line should be 0.276 if both lines are formed in LTE. Except for NGC 2024, these values, given in Table 4, show that the ratio is more than 3σ below the LTE value and non-LTE effects are present. The usual interpretation has been that the H 109α lines more strongly stimulated than the H 137β lines and that the T_e^* values obtained from the H 137β lines are closer to the true electron temperature. Although Lockman and Brown (1976) have pointed out that geometrical effects might affect these β to α ratios for a spherical H II region with variable density and electron temperature, the unpublished data of Churchwell et al. show no such effects in Orion A, and in the following we will assume that a plane-parallel geometry accurately represents the source structure.

The most surprising result of the comparison is the agreement of the T_e^*'s from the H 66α and H 109α data, because the H 66α emission is weighted toward dense gas which is close to LTE, while the H 109α emission is weighted towards more diffuse ionized gas which is affected by stimulated emission. A detailed investigation of a possible causal relationship between the T_e^*'s values can be carried out only for Orion A, where we have enough data. From the H 66α (Pauls and Wilson, 1977), and H 109α (Churchwell et al.) data there are no large temperature gradients in this source. Hence the true electron temperature of the H 109α line formation region is $\sim$7000–8000 K. However, to have T_e^* equal the true electron temperature, stimulated emission, which lowers T_e^* must be balanced by pressure broadening. Pressure broadening shifts some of the line intensity into broad, weak wings, which are on the order of the noise. These wide wings are lost in the baseline fits and hence the T_e^* is raised. Both effects, stimulated emission and pressure broadening may be on the order of 10–20% of the line intensity, and it seems that the agreement of T_e^* (H 66α) and T_e^* (H 109α) is caused by the fact that both effects are the same size. To obtain the necessary amount of collisional broadening, the true electron density must be more than twice the r.m.s. electron density. Hence the clumping factor, which is the square of ratio of the electron densities, is more than 4, and only 25% of the nebula is filled with ionized gas of density $>10^4$ cm^{-3}. The large clumping factor is in agreement with estimates obtained from optical observations.

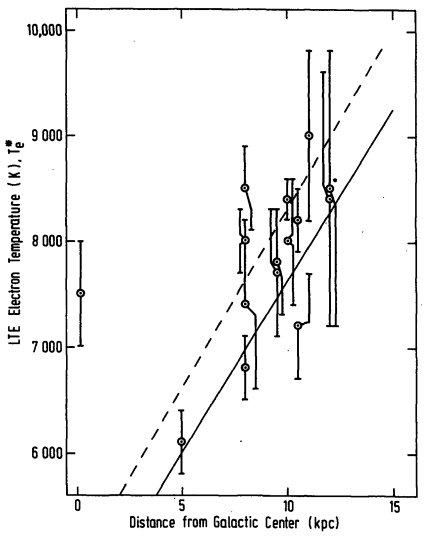

Fig. 2. The H 66α LTE Electron Temperatures obtained from our H 66α line data plotted against distance from the galactic center. The average LTE Electron Temperature, weighted inversely by the square of the error is 7900 K. The two sources located within 5 kpc of the galactic center are W 33 and Sgr B 2. For these sources the true electron temperature may be significantly different from T_e^*, either because of stimulated emission or because of optical depth effects. The dotted line gives the average value of the LTE Electron Temperature obtained by Churchwell et al. from their 137β line data, and the solid line is the corresponding Electron Temperature obtained from the H 109α line data

Radial Gradients in T_e^* in the Galaxy

Fig. 2 shows our T_e^* plotted as a function of distance from the galactic center. We also show the gradient in T_e^* obtained by Churchwell et al. for the H 109α and H 137β T_e^*'s. Our data do not cover a large enough range in distance from the galactic center to test the H 109α results of Churchwell et al., but the H 66α results are consistent with the gradient in LTE electron temperature with distance from the galactic center given by Churchwell et al.

Acknowledgement. We thank P. Shaver and especially C. M. Walmsley for helpful criticism. E. Churchwell and C. M. Walmsley kindly provided unpublished data and also the computer program used to calculate the model electron temperatures.

Appendix

Notes to Table 1

W 3A and W 3B. These are the two strongest sources in the continuum complex W 3. These sources are barely separated by our beam. W 3A has a shell structure and W 3B has a gaussian-like shape. On the basis of an H 109α aperture synthesis map, Wellington et al. (1976) had claimed that the radial velocities if W 3A and B were significantly different. Our H 66α velocities, however, are equal to within the uncertainties. For the corrections to the electron temperature (col. 12, Table 1), we took the angular size of W 3B, 17″, from Wynn-Williams (1971).

Orion A and Ori A (1.6′*S*). These are the two prominent peaks in the Orion H II region. The region around the peak of Orion A has been mapped by Pauls and Wilson (1977). The second peak, 1.6′ south of the main source, is a newly detected object and its nature is unknown. This second peak is present in the interferometer map of Martin and Gull (1976), but is not prominent on optical photographs.

NGC 2024. The flux density of this source is considerably lower than 55 Jy, the flux density obtained by integrating maps of the source (Schraml and Mezger, 1969; Shaver and Goss, 1970). The difference in the flux density is caused by our low values of the angular size. Because the source has at least two components, our parameters may refer only to the denser one.

Mon R 2. Our angular size and flux density is consistent with the value given by Downes et al. (1975). The lower limit to the central emission measure at 10.7 GHz given by Downes et al., 7.4 10^6 cm^{-6} pc, would cause 7% stimulated emission at 22 GHz. However it is possible that the source is somewhat optically thick at 10.7 GHz, and even higher emission measure components are present.

Sgr B 2. Our data refer to one set of components in this complex, that refered to as sources 3 and 5 by Martin and Downes (1972). A second component called source 4 by Martin and Downes, 1′ north of this source, has a radial velocity of 70.8 ± 0.8 km s^{-1}. The rapid change indicates that large velocity gradients are present in the H II region. We did not include the second component in Table 1 because of uncertainties in the continuum data. Our flux density is about 10 times that reported by Martin and Downes, but our flux estimates undoubtedly include a large contribution from the smooth background, not present in the interferometer map. We follow Reifenstein et al. (1970) in assuming that the Sgr B 2 complex is 200 pc from the galactic center.

W 33. This is the dense component in the H II region complex. We have used the distance to the source presented by Gardner et al. (1975), and the angular size of $\sim 14'' \times \sim 27''$, given by Goss et al. (1977). Our flux density agrees well with the 10.7 GHz value of Goss et al.

M 17. Our data refer only to the southern peak in this source, hence our flux densities and angular sizes, etc. do not represent values for the entire nebula. The flux density of the entire nebula is 609 Jy (Schraml and Mezger, 1969).

W 49. Our data refer to the dense components 5 and 6 of Wynn-Williams (1971). The size for component 6 used in the calculation of the source optical depth, was taken from Wynn-Williams (1971). The trend in the radial velocities, i.e. increasing radial velocity with increasing Right Ascension, is in agreement with the lower-resolution results of Gordon and Wallace (1971).

W 51. The source numbering was taken from the interferometer map of W 51 by Martin (1972). Radial velocities measured with an angular resolution of 4′ showed that this, the northern part of the W 51 complex, had velocities below 60 km s^{-1}, while the group of sources 24′ SW had radial velocities above 68 km s^{-1}. Using this information, Wilson et al. (1970) has proposed that the W 51 region consists of two independent groups of sources, at 7 and 8.5 kpc from the Sun. Component *B*, for which the H 66α line velocity is 66.2 km s^{-1}, is located in the group which exhibited velocities of 58 km s^{-1} in the data of Wilson et al. This might indicate that peculiar velocities in this region are ~ 12 km s^{-1}, and the simple model of Wilson et al. should be revised. The flux densities reported by Martin (1972) for component *B* agree to within 30% of our value. However, our flux densities for components *D* and *E* exceed Martin's by factors of 3 and 1.5, respectively. As Martin points out, these sources are optically thick between 2.7 and 5 GHz, where he obtained the flux density data, but a larger contribution may come from a smooth background which is resolved by the interferometer.

K 3–50. Our data refer to the northernmost compact component in this complex. This component is refered to as K 3–50 C, and is resolved into two components with a 2″ resolution (Harris, 1975). Our flux density agrees with the 5 GHz value of Harris (1975), and we have used the average of the angular sizes of the components listed by Harris in our computation of the corrected electron temperature. Unpublished H 90α data of Wilson and Jaffe made with a resolution of 90″, do not show the H 66α velocity, but rather a range of radial velocities between −29 and −23 km s^{-1}. However K 3–50 C is compact and dilution in the 90″ beam would be significant. This component is located within 10″ of the 1720 MHz OH maser center in K 3–50, and the radial velocity of the H 66α line is within 3 km s^{-1} of the velocity of the OH line.

DR 21. Our data probably refer to the components *A*, *B*, and *C* in the interferometer map of Harris (1973). Our value of the LTE electron temperature, T_e^*, agrees very well with the T_e^* obtained from an analysis of the radio continuum flux densities measured at various frequencies (see e.g. Salem and Seaton, 1974). Although our flux density agrees very well with that reported at lower frequencies by Harris (1975), the line width, 43 km s^{-1}, and radial velocity, −2.5 km s^{-1}, of the recombination lines measured at 5 GHz (Churchwell et al.) differ from our values by much more than the quoted errors. Hence the 5 GHz recombination lines may be formed in a completely different region.

References

Brocklehurst, M.: 1970, *Monthly Notices Roy. Astron. Soc.* **148**, 417

Brocklehurst, M., Seaton, M. J.: 1972, *Monthly Notices Roy. Astron. Soc.* **157**, 179

Berulis, I. I., Smirnov, G. T., Sorochenko, R. L.: 1975, *Soviet Astron. Letters* **1**, 187

Brown, R. L., Lockman, F. J., Knapp, G. R.: 1979, *Ann. Rev. Astron. Astrophys.* (in press)

Churchwell, E., Smith, L. F., Mathis, J., Mezger, P. G., Huchtmeier, W.: 1979, *Astron. Astrophys.* **70**, 719

Downes, D., Winnberg, A., Goss, W. M., Johansson, E. B.: 1975, *Astron. Astrophys.* **44**, 243

Gardner, F. F., Wilson, T. L., Thomasson, P.: 1975, *Astrophys. Letters* **16**, 29

Gordon, M. A., Wallace, D.: 1971, *Astrophys. J.* **167**, 235

Goss, W. M., Matthews, H. E., Winnberg, A.: 1978, *Astron. Astrophys.* **65**, 307

Harris, S.: 1973, *Monthly Notices Roy. Astron. Soc.* **162**, 5p

Harris, S.: 1975, *Monthly Notices Roy. Astron. Soc.* **170**, 139

Lockman, F. J., Brown, R. L.: 1976, *Astrophys. J.* **207**, 436

Martin, A. H. M.: 1972, *Monthly Notices Roy. Astron. Soc.* **157**, 31

Martin, A. H. M., Downes, D.: 1972, *Astrophys. Letters* **11**, 219

Martin, A. H. M., Gull, S. F.: 1976 *Monthly Notices Roy. Astron. Soc.* **179**, 217

Pauls, T., Wilson, T. L.: 1977, *Astron. Astrophys.* **60**, L31

Reifenstein, E. C. III, Wilson, T. L., Burke, B. F., Mezger, P. G., Altenhoff, W. J.: 1970, *Astron. Astrophys.* **4**, 357

Salem, M., Seaton, M. J.: 1974, *Monthly Notices Roy. Astron. Soc.* **167**, 493

Schraml, J., Mezger, P. G.: 1969, *Astrophys. J.* **156**, 269

Shaver, P. A., Goss, W. M.: 1970, *Australian J. Phys. Astrophys. Suppl.* **14**, 133

Waltman, E. B., Johnston, K. J.: 1973, *Astrophys. J.* **182**, 489

Wellington, K. J., Sullivan, W. T. III, Goss, W. M., Matthews, H. E.: 1976, *Astron. Astrophys.* **47**, 351

Wilson, T. L., Mezger, P. G., Gardner, F. F., Milne, D. K.: 1970, *Astrophys. Letters* **5**, 99

Wynn-Williams, C. G.: 1971, *Monthly Notices Roy. Astron. Soc.* **151**, 397